Title

Multispectral Optoacoustic Tomography of Muscle Perfusion and Oxygenation under Arterial and Venous Occlusion – A Human Pilot Study

Authors

Angelos Karlas, MD[1,2,3,5+], Michael Kallmayer, MD[3,+], Nikolina-Alexia Fasoula, MD[1,2], Evangelos Liapis, PhD[1,2], Michail Bariotakis, PhD[1,2], Markus Krönke, MD[4], Maria Anastasopoulou, MS[1,2], Josefine Reber, PhD[1,2], Hans-Henning Eckstein, MD[3,5], Vasilis Ntziachristos, PhD[1,2,5,*]

[1] Chair for Biological Imaging, Center for Translational Cancer Research (TranslaTUM), Technical University of Munich, Klinikum rechts der Isar, Munich, Germany, [2] Helmholtz Zentrum München, Institute of Biological and Medical Imaging, Neuherberg, Germany, [3] Clinic of Vascular and Endovascular Surgery, Technical University of Munich, Klinikum rechts der Isar, Munich, Germany, [4] Clinic of Nuclear Medicine, Technical University of Munich, Klinikum rechts der Isar, [5] DZHK (German Centre for Cardiovascular Research), partner site Munich Heart Alliance, Munich, Germany, [+] Equal Contribution, * Corresponding Author: v.ntziachristos@gmail.com.

Article Type: Brief Report

This article has been accepted for publication and undergone full peer review but has not been through the copyediting, typesetting, pagination and proofreading process which may lead to differences between this version and the Version of Record. Please cite this article as doi: 10.1002/jbio.201960169

Total Word Count:

Subject Terms:
Ischemia, Thrombosis, Peripheral Arterial Disease, Photoacoustics, Muscle Metabolism

Abstract

Objective: Perfusion and oxygenation are critical parameters of muscle metabolism in health and disease. They have been both the target of many studies, in particular using Near-Infrared Spectroscopy (NIRS). However, difficulties with quantifying NIRS signals have limited a wide dissemination of the method to the clinics. Our aim was to investigate whether clinical Multispectral Optoacoustic Tomography (MSOT), could enable the label-free imaging of muscle perfusion and oxygenation under clinically relevant challenges: the arterial and venous occlusion.

Approach and Results: We employed a hybrid clinical MSOT/Ultrasound system equipped with a hand-held scanning probe to visualize hemodynamic and oxygenation changes in skeletal muscle under arterial and venous occlusions. Four (N=4) healthy volunteers were scanned over the forearm for both 3-minute occlusion challenges. MSOT recorded pathophysiologically expected results during tests of disturbed blood flow with high resolution and without the need for contrast agents. During arterial occlusion, MSOT-extracted Hb-values showed an increase, while HbO2- and TBV-values remained roughly steady, followed by a discrete increase during the hyperemic period after cuff deflation. During venous occlusion, results showed a clear increase in intramuscular HbO_2, Hb and TBV within the segmented muscle area.

Conclusions: MSOT was found to be capable of label-free non-invasive imaging of muscle hemodynamics and oxygenation under arterial and venous occlusion. We introduce herein

MSOT as a novel modality for the assessment of vascular disorders characterized by disturbed blood flow, such as acute limb ischemia and venous thrombosis.

Introduction

Muscle perfusion and oxygenation (MOx) are key component of muscle metabolism affected in several diseases, including peripheral arterial disease (PAD), deep vein thrombosis (DVT), heart failure, and diabetes mellitus[1-5]. Non-invasive perfusion and MOx measurements are desirable for quantifying parameters associated with fitness level, disease severity and therapy efficacy. Traditional methods of measuring these parameters, such as the ultrasound, the magnetic resonance spectroscopy (MRS) and imaging (MRI), or nuclear medicine techniques (e.g. positron emission tomography, PET) have limitations that impair direct testing of muscle function and their application to large-scale studies: they do not provide direct MOx information, are costly or employ ionizing radiation.

Near-infrared spectroscopy (NIRS) and diffuse optical tomography (DOT) have been investigated as techniques for high-throughput non-invasive and label-free assessment of MOx and muscle hemodynamics in real-time [6-8]. NIRS allows for direct sensing and differentiation of oxy- (HbO_2) and deoxy-hemoglobin (Hb) and was thus introduced as a technique for imaging hemodynamics and oxygen of soft tissues. Furthermore, NIRS reaches depths of several centimeters, due to the low attenuation of light at infrared wavelengths. While the HbO_2- and

Hb-contrast achieved by NIRS and DOT is indeed valuable for the assessment of metabolic function, there are significant limitations in the quantitative accuracy and the resolution achieved [9]. Their fundamental limit comes from the strong photon scattering in tissues, which generates uncertainty in the information collected. In fact, it is challenging to extract the individual contributions of Hb and HbO_2 from the measured scattering alterations in tissues and thus to achieve quantification of hemoglobins. Moreover, the techniques offer very low spatial resolution, mixing contributions from muscle and more superficial tissues such as the fat and the skin. Until today, neither NIRS nor DOT have found widespread acceptance in the clinics [10, 11].

Optoacoustic imaging is a high-resolution method that solves the fundamental limitations of purely optical imaging by using ultrasonic instead of optical detection, making it insensitive to photon scattering. The method has been employed to image peripheral arteries [12, 13], arteriovenous malformations [14], breast cancer [15], systemic sclerosis [16], Crohn's disease [17] or brown fat activation over time [18]. Optoacoustic imaging has also shown ability to perform monitoring of hemodynamic responses after exercise in healthy volunteers [19]. A next step with clinical relevance is to examine whether the method could image hemodynamics and oxygenation changes under conditions typical of blood flow disturbances, such as arterial and venous occlusion.

Our purpose was to investigate whether clinical optoacoustics, in particular Multispectral Optoacoustic Tomography (MSOT), could enable the label-free imaging of muscle perfusion and oxygenation under conditions of arterial and venous occlusion, which simulate the acute limb ischemia and the venous thrombosis correspondingly.

Methods

Study design and experimental protocol

All healthy volunteers consented to participate in the measurements in full accordance with the work safety regulations of the Helmholtz Center Munich (Neuherberg, Germany). All four (N=4, 2 males, 2 females, age mean 36, range 33-37) subjects were non-smokers. They were asked to avoid consuming caffeine, food, and alcohol for at least 8h before the planned measurements.

Tests took place in a dark, quiet room with an average temperature of ~24°C over the whole duration of the recordings. Subjects sat with their arms at heart-level. After five minutes of rest, the blood pressure of each subject was measured three times to confirm that all were normotensive. For the venous occlusion challenge, the cuff was inflated to a pressure of 80 mmHg. For the arterial occlusion challenge, the cuff was inflated up to 40 mmHg above the subject's systolic blood pressure (SBP), as extracted by the mean value of the three blood pressure readings. The MSOT probe was applied along the forearm and over the brachioradialis

muscle identified by anatomic knowledge and after activating it by handgrip contractions under real-time ultrasound imaging (Figure 1).

Handheld multispectral optoacoustic imaging

Measurements were conducted using a hybrid clinical MSOT/Ultrasound system (Acuity©, iTheraMedical GmbH, Munich, Germany) equipped with a handheld scanning probe. The system was able to acquire real-time optoacoustic and ultrasound data simultaneously at a framerate of 25 Hz for the optoacoustic data and ~9Hz for the ultrasound data. The casing of the handheld probe was 3D-printed offering decreased weight and increased flexibility and freedom to the operator (Figure 1a). The water tank was filled with heavy water (D_2O) which is characterized by less light absorption at the near-infrared range, compared to the normal water, while providing ideal coupling of the ultrasound waves in tissue in response to light absorption. The hand-held probe was equipped with 256 piezoelectric elements with a central frequency of 4MHz arranged in an arc of 145° for ultrasound detection. Illumination was delivered to tissue through an optical fiber, which was mounted on the same hand-held probe. Illumination was delivered in the form of short light pulses (~10ns in duration), at a rate of 25Hz. For each pulse, almost 15mJ of energy were delivered over a rectangle area of around 1x4cm, which is far below the safety limits of laser use for medical applications [20]. For multispectral image acquisition, we employed 28 different light wavelengths (from 700 to

970nm at steps of 10nm). All acquired optoacoustic data were further reconstructed using a model-based reconstruction method published before [21].

Image segmentation, analysis and visualization

Muscle segmentation was done by means of a custom-made semi-automated algorithm based on active contours [22]. For each venous or arterial occlusion recording, a muscle ROI was manually delimited in a single image used for the initialization of the semi-automated algorithm. This was performed after building consensus between two clinicians with extensive experience in clinical ultrasound and MSOT imaging. For each initialization image the muscle was first visually identified in the corresponding and co-registered ultrasound image, based on previous knowledge of the local anatomy and the characteristic texture of muscle in ultrasound. Then, a curved ROI was manually delineated directly on the initialization image: an addition of the optoacoustic image corresponding to the 800 nm, which represents the TBV, and the one corresponding to the 970 nm, which represents the water tissue content. This way we ensured that the decision of the two clinicians was based more on functional and physiological information, taking into account that the skeletal muscle is a highly perfused and hydrated tissue, and less on purely morphological information, provided by ultrasound. Manual segmentation of the muscle was repeated three times to ensure consistency of results, based on three different initialization images: one corresponding to the resting period before the

occlusion, one corresponding to the occlusion period and one corresponding to the resting period after the end of occlusion. For each of the three readouts a value for the HbO_2-, Hb- or TBV-level for each MSOT frame was extracted by averaging the absorption values of all pixels within the muscle ROI for this frame. Thus: i. The Hb-points were extracted from the sequence of the successive 750 nm-frames, ii. The TBV-signal were extracted from the successive 800 nm-frames and iii. The HbO_2-signal were extracted from the successive 850 nm-frames. Finally, the mean value of the three readouts for each time point was plotted as the HbO_2-, Hb- or TBV-level for this time point. The per subject baseline value for each physiological parameter (Hb, HbO_2 or TBV) was calculated as the average of all the plotted values over the first 30 seconds of the recording before the inflation of the occlusion cuff.

The manual segmentation of the initialization image resulted in an initial binary image with the pixels belonging to the muscle ROI having non-zero intensity (white) and all other background pixels having zero intensity (black). Subsequently, a binary image was automatically calculated for each multispectral stack (28 recorded single-wavelength frames from 700 to 970 nm at steps of 10 nm) throughout each recording based on the binary image or muscle ROI corresponding to the previous one. The rules controlling the calculation of each binary image, or the muscle ROI from the previous image, were regulated by the principle of the active contours, which aims at minimizing the energy defined by the forces tending to expand the contour (imaged intensity-based) and the ones tending to shrink it (smoothing-based). Taking

into account the absence of significant motion throughout the whole recording, the evolution of the active contour or muscle ROI was smooth. All calculations and quantifications took place on the raw optoacoustic images. For visualization purposes, all images were denoised and lightly contrast-enhanced to the same extent.

Results

Venous occlusion challenge

The venous occlusion challenge in human volunteers shows an increase of muscle Hb, HbO_2 and TBV during the occlusion due to the obstruction of the forearm venous outflow, while maintaining an arterial inflow. The maximum median Hb-increase from the baseline is observed at the 3rd or last minute of venous occlusion (+30.91% compared to baseline). After the cuff deflation the Hb-signal shows a radical decrease of -21.44%, reaching a level of + 9.47% compared to baseline, as demonstrated in the image series of Fig. 2a. Accordingly, the maximum median increase of the HbO_2 (+27.54%) and TBV signal (+27.64%) over the scanned muscle, compared to the subject's baseline, are observed at the 2nd minute after cuff inflation. All measured optoacoustic signals return to roughly baseline levels after the end of venous occlusion. With reference to hemodynamics (TBV fluctuations) and dynamics of HbO_2 and Hb,

an indicator of intramuscular oxygen kinetics, our median venous occlusion readouts showed the fluctuations presented in Table 1.

Table 1. Venous occlusion challenge: Total fluctuations of TBV, HbO_2 and Hb compared to the baseline, along with per-minute percentage changes (Δ) for all healthy volunteers.

Time	TBV		HbO_2		Hb	
	Δ	Total	Δ	Total	Δ	Total
1st minute of occlusion	+11.11%	+11.11%	+14.32%	+14.32%	+ 8.69%	+8.69%
2nd minute of occlusion	+16.53%	+27.64%	+ 13.22%	+27.54%	+16.69%	+25.38%
3rd minute of occlusion	-2.99%	+24.65%	- 5.07%	+22.47%	+ 5.53%	+30.91%
1st minute after cuff deflation	-11.23%	+13.42%	- 7.77%	+14.7%	-21.44%	+9.47%
2nd minute after cuff deflation	- 2.76%	+10.66%	- 3.44%	+11.26%	-3.61%	+5.86%

These trends are represented visually in Figure 2. Figure 2a depicts the MSOT image series of the Hb-distribution within the forearm muscle of Subject 3 for each minute of the venous occlusion challenge. All images correspond to the 750 nm light wavelength, where light absorption of Hb is critically higher than that of HbO_2. Figures 2b and 2c depict the corresponding MSOT image series for the HbO_2- and TBV-distributions in the forearm muscle of the same subject. The HbO_2 images correspond to 850 nm, where HbO_2 light absorption is higher than that of Hb, and the TBV images to 800 nm light wavelength, which is the isosbestic point of Hb, and HbO_2, where the absorptions of the two hemoglobins are equal. The

observable fluctuations in the images are in line with the quantitative measures of hemodynamics and oxygenation plotted in Figure 2d for Subject 3.

Figure 2e summarizes the statistics of the Hb-levels during the venous occlusion test for the whole group of participating subjects (n=4). Correspondingly, the box plots of Figure 2f and Figure 2g present the statistics of the HbO_2- and TBV-levels during the venous occlusion challenge for all subjects. The marked median values for the sample represent the central trend of change in relation to the per-subject baseline. These are calculated from the four average intensities of the optoacoustic signal in the muscle ROI during each minute of the challenge.

Arterial occlusion challenge

The MSOT recordings during the arterial occlusion challenge showed a restriction in muscle perfusion and oxygenation with a clear rebound effect after the release of the cuff occlusion or else during the hyperemia period.

As observed, during the arterial occlusion there is an increase in the intramuscular Hb-signal (+14.9% compared to baseline at 3 minutes after cuff inflation) with a decrease (-13.01%) after cuff deflation, reaching a level of only +1.89% above the baseline. On the contrary, the HbO_2-signal remains roughly stable or decreases in selected cases (e.g. Subject 3) during the arterial occlusion and prominently increases during the postocclusive hyperemic period (+13.68% at 1 minute after cuff deflation). Only minor fluctuations are observed for the median value of the

corresponding intramuscular TBV-signal over the complete arterial occlusion challenge. The total MSOT readouts for the hemodynamics and oxygen kinetics during the arterial occlusion challenge showed (Table 2):

Table 2. Arterial occlusion challenge: Total fluctuations of TBV, HbO_2 and Hb compared to the baseline along with per-minute percentage changes for all healthy volunteers.

Time	TBV		HbO_2		Hb	
	Δ	Total	Δ	Total	Δ	Total
1st minute of occlusion	+ 7.39%	+ 7.39%	+ 5.96%	+ 5.96%	+ 9.11%	+ 9.11%
2nd minute of occlusion	- 2.01%	+5.38%	+ 0.09%	+6.05%	- 1.12%	+7.99%
3rd minute of occlusion	+ 3.97%	+9.35%	+ 2.19%	+8.24%	+ 6.91%	+14.9%
1st minute after cuff deflation	+ 0.14%	+9.49%	+ 5.44%	+13.68%	- 13.01%	+1.89%
2nd minute after cuff deflation	- 0.96%	+8.53%	- 5.47%	+8.21%	+ 2.98%	+4.87%

The aforementioned trends can be inspected visually in Figure 3. Figure 3a depicts representative MSOT images of the Hb-distribution (750nm) over the examined muscle for each minute of the arterial occlusion challenge (Subject 3). Figure 3b and Figure 3c show the MSOT

image series for the HbO_2 (at 850nm) and TBV (at 800nm) intramuscular distributions of the same subject on a per-minute basis. Figure 3d shows the fluctuations of the mean values of Hb- (blue line), HbO_2- (magenta line) and TBV-signal (orange line) within the muscle region of interest. Figure 3e depicts the statistics of the Hb-levels during the arterial occlusion test for the group of examined healthy volunteers. Furthermore, Figure 3f and Figure 3g show the box plots for HbO_2- and TBV-kinetics during the 3-minute arterial occlusions for all (n=4) subjects. The per-minute median values represent again the change from the baseline for each subject and are extracted from the mean values of optoacoustic signal over the muscle region during each minute of the test.

Discussion

The assessment of peripheral muscle hemodynamics and oxygenation during vascular occlusions is important for monitoring a spectrum of diseases relating to peripheral vascular function or systemic cardiovascular sufficiency. Different tests exist to assess aspects of insufficient blood supply and oxygenation, including from simple visual observation for signs of cyanosis, pulse oximeter measurements of arterial blood saturation, and blood flow profiling using Doppler ultrasound. Nevertheless, no established clinical test today measures directly the oxygenation and secondary the perfusion of certain organs.

Because the aforementioned techniques, such as the ultrasound, the magnetic resonance and the nuclear medicine techniques, make use of indirect measurements, they fail to meet several critical clinical needs. These could include the objective quantification of PAD severity, the effect of systemic conditions such as heart failure or chronic obstructive pulmonary disease on peripheral muscle oxygen delivery, or even the early detection of septic shock by monitoring peripheral tissue hemodynamics.

By conducting targeted measurements on healthy volunteers, we demonstrate herein the capability of clinical hand-held MSOT to record pathophysiologically expected results during tests of disturbed blood flow with high spatial and temporal resolution and without the need for contrast agents. Thus, by resolving spatial and temporal hemoglobin gradients, MSOT could serve as a novel tool for imaging muscle hemodynamics and oxygenation during several functional challenges, which affect blood flow, such as the venous occlusion as the one developed in venous thrombosis or the arterial occlusion developed in peripheral arterial disease or critical limb ischemia. For example, the arterial occlusion challenge conducted here is a well-established method for the non-invasive assessment of microvascular endothelial dysfunction in soft tissues such as the muscle or the skin: an indicator of increased risk for developing cardiovascular and metabolic disease [23-25].

Our recordings during arterial and venous occlusion challenges showed pathophysiologically expected results, as reported by means of alternative methods for measuring soft tissue

hemodynamics and oxygenation [26, 27]. During cuff-induced venous occlusion, a condition simulating CVI or DVT, the cuff pressure (80 mmHg) blocks the venous drainage of the forearm leaving the arterial inflow unaffected and leading to an increase in the forearm volume. MSOT-recorded values showed a clear increase in intramuscular HbO_2, Hb and TBV within the segmented muscle area. Our results comply with reported measurements conducted by means of other label-free methods, such as the NIRS and the venous occlusion plethysmography (VOP), a method used to estimate the limb blood flow, based on the changes in the limb volume under cuff-induced venous occlusion [28, 29].

However, clinical MSOT is capable of providing not only precise one-dimensional time-series measurements, as usually provided by other methods, but also high-resolution (approximately 250μm) tomographic images of the muscle tissue with additional spatial maps of perfusion and oxygenation in real-time. Of importance herein is the ability to differentiate depth (up to 3-4cm) in contrast to diffuse optical methods, due to the higher resolution achieved. This capacity makes MSOT much more accurate than optical imaging or spectroscopy methods, because in MSOT muscle-specific contributions can be quantified based on image guidance. As seen in the morphological images of muscle, optoacoustic imaging can clearly delineate tissue structures, allowing for precisely targeted measurements. This is an important strength over diffuse optical methods characterized by positional uncertainty due to the significant image blurring and the ill-posed nature of the quantitative problem solved.

During cuff-induced arterial occlusion, a condition simulating PAD, the cuff pressure (40 mmHg above individual's systolic blood pressure, SBP) blocks the arterial inflow and the venous drainage of the forearm leaving essentially unaffected the forearm volume. During arterial occlusion measurements, the MSOT-extracted Hb-value showed an increase, revealing a deoxygenation of the muscle tissue due to complete cessation of the inflow of oxygenated arterial blood. Although arterial occlusion was expected to lead to a prominent decrease in intramuscular HbO_2 for all participants, our results showed a decrease in selected cases (e.g. Subject 3) but a roughly steady HbO_2 across the whole cohort. It has been shown in the past that cuff inflation even at pressures significantly higher than the SBP could lead to subtotal arterial occlusion and a state of arterial low flow during the cuff-on period [30]. Even under this condition, it is the abrupt increase of the flow-induced wall shear stress after the cuff deflation which stimulates the vascular endothelium to produce and secrete nitric oxide, a potent vasodilatatory molecule that leads to tissue hyperemia [31]. MSOT was capable of detecting and quantifying this phenomenon, showcasing high sensitivity since it can give reliable readouts even under subtotal arterial occlusion where low flow and not total ischemia is present.

Even if MSOT shows great potential for imaging muscle perfusion and oxygenation, it does not come without limitations. Due to light attenuation effects (scattering and absorption) with increasing depth, MSOT is characterized by low penetration (3-4 cm) compared to other clinical imaging modalities. Furthermore, the spectral unmixing of multispectral optoacoustic data is

error-prone because of the 'spectral colouring' effect or else the deviation of the measured absorption spectrum of a deep-lying light absorber (e.g. Hb) from its known spectrum due to light-tissue interactions before the illumination light reaches it. Even if solutions have been presented for preclinical MSOT data [32], this effect hampers the absolute quantification of light absorbers in living tissues and remains a challenging problem for clinical MSOT imaging. To avoid such sources of error, all calculations presented in the current study were performed on raw measured MSOT data.

We presented herein the first, to our knowledge, attempt to record precise tomographic images of intramuscular hemodynamic and oxygenation phenomena during periods of disturbed blood flow. MSOT provided pathophysiologically expected results without the need for injected contrast agents, increasing patient convenience and decreasing costs. Furthermore, MSOT measurements did not require special subject and equipment preparation and may be easily incorporated into daily clinical routine opening up to new possibilities for clinical metabolic imaging of normal or dysfunctional muscle. Our work displays the capacity of MSOT in tracking such phenomena, suggesting it as a research and clinical imaging tool to investigate exercise muscle physiology, peripheral and systemic diseases such as PAD or heart failure, as well as metabolic diseases, such as diabetes mellitus. Subsequent focused studies will advance MSOT towards clinical translation, which will impact objective diagnostics and evaluation of applied pharmacological or interventional therapies.

Sources of Funding

This project has received funding from the European Research Council (ERC) under the European Union's Horizon 2020 research and innovation programme under grant agreement No 694968 (PREMSOT) and was supported by the DZHK (German Centre for Cardiovascular Research) and by the BMBF (German Ministry of Education and Research) and by the Helmholtz Zentrum München, funding program "Physician Scientists for Groundbreaking Projects".

Disclosures

V. Ntziachristos has stock/stock options in iThera Medical. All other authors have no conflicts of interest to declare.

References

1. Brass EP, Hiatt WR and Green S. Skeletal muscle metabolic changes in peripheral arterial disease contribute to exercise intolerance: a point-counterpoint discussion. *Vasc Med*. 2004;9:293-301.
2. Poole DC, Hirai DM, Copp SW and Musch TI. Muscle oxygen transport and utilization in heart failure: implications for exercise (in)tolerance *American journal of physiology Heart and circulatory physiology*; 2012(302): H1050-63.

3. Gibson CM, Cannon CP, Daley WL, Dodge JT, Alexander B, Marble SJ, McCabe CH, Raymond L, Fortin T, Poole WK, Braunwald E and Group ftTS. TIMI Frame Count : A Quantitative Method of Assessing Coronary Artery Flow. *Circulation*. 1996;93:879-888.
4. Gschwandtner ME and Ehringer H. Microcirculation in chronic venous insufficiency. *Vasc Med*. 2001;6:169-79.
5. Liu K, Chen LE, Seaber AV, Johnson GW and Urbaniak JR. Intermittent pneumatic compression of legs increases microcirculation in distant skeletal muscle. *Journal of orthopaedic research : official publication of the Orthopaedic Research Society*. 1999;17:88-95.
6. Durduran T, Choe R, Baker WB and Yodh AG. Diffuse Optics for Tissue Monitoring and Tomography. *Rep Prog Phys*. 2010;73.
7. Hamaoka T, McCully KK, Quaresima V, Yamamoto K and Chance B. Near-infrared spectroscopy/imaging for monitoring muscle oxygenation and oxidative metabolism in healthy and diseased humans. *J Biomed Opt*. 2007;12:062105.
8. Gibson A and Dehghani H. Diffuse optical imaging. *Philosophical transactions Series A, Mathematical, physical, and engineering sciences*. 2009;367:3055-72.
9. Strangman G, Franceschini MA and Boas DA. Factors affecting the accuracy of near-infrared spectroscopy concentration calculations for focal changes in oxygenation parameters. *Neuroimage*. 2003;18:865-79.
10. Boas DA, Dale AM and Franceschini MA. Diffuse optical imaging of brain activation: approaches to optimizing image sensitivity, resolution, and accuracy. *Neuroimage*. 2004;23 Suppl 1:S275-88.
11. Kek KJ, Kibe R, Niwayama M, Kudo N and Yamamoto K. Optical imaging instrument for muscle oxygenation based on spatially resolved spectroscopy. *Optics express*. 2008;16:18173-87.
12. Karlas A, Reber J, Diot G, Bozhko D, Anastasopoulou M, Ibrahim T, Schwaiger M, Hyafil F and Ntziachristos V. Flow-mediated dilatation test using optoacoustic imaging: a proof-of-concept. *Biomed Opt Express*. 2017;8:3395-3403.
13. Karlas A, Fasoula NA, Paul-Yuan K, Reber J, Kallmayer M, Bozhko D, Seeger M, Eckstein HH, Wildgruber M and Ntziachristos V. Cardiovascular optoacoustics: From mice to men - A review. *Photoacoustics*. 2019;14:19-30.
14. Masthoff M, Helfen A, Claussen J, Karlas A, Markwardt NA, Ntziachristos V, Eisenblatter M and Wildgruber M. Use of Multispectral Optoacoustic Tomography to Diagnose Vascular Malformations. *JAMA dermatology*. 2018.
15. Diot G, Metz S, Noske A, Liapis E, Schroeder B, Ovsepian SV, Meier R, Rummeny E and Ntziachristos V. Multispectral Optoacoustic Tomography (MSOT) of Human Breast Cancer. *Clinical cancer research : an official journal of the American Association for Cancer Research*. 2017;23:6912-6922.
16. Masthoff M, Helfen A, Claussen J, Roll W, Karlas A, Becker H, Gabriels G, Riess J, Heindel W, Schafers M, Ntziachristos V, Eisenblatter M, Gerth U and Wildgruber M. Multispectral optoacoustic tomography of systemic sclerosis. *J Biophotonics*. 2018;11:e201800155.
17. Knieling F, Neufert C, Hartmann A, Claussen J, Urich A, Egger C, Vetter M, Fischer S, Pfeifer L, Hagel A, Kielisch C, Gortz RS, Wildner D, Engel M, Rother J, Uter W, Siebler J, Atreya R, Rascher W, Strobel D, Neurath MF and Waldner MJ. Multispectral Optoacoustic Tomography for Assessment of Crohn's Disease Activity. *N Engl J Med*. 2017;376:1292-1294.

18. Reber J, Willershäuser M, Karlas A, Paul-Yuan K, Diot G, Franz D, Fromme T, Ovsepian SV, Bézière N, Dubikovskaya E, Karampinos DC, Holzapfel C, Hauner H, Klingenspor M and Ntziachristos V. Non-invasive Measurement of Brown Fat Metabolism Based on Optoacoustic Imaging of Hemoglobin Gradients. *Cell Metabolism*. 2018;27:689-701.e4.
19. Diot G, Dima A and Ntziachristos V. Multispectral opto-acoustic tomography of exercised muscle oxygenation. *Opt Lett*. 2015;40:1496-9.
20. America. TLIo. American national standards for the safe use of lasers. *ANSI Z1361*. 2000.
21. Rosenthal A, Ntziachristos V and Razansky D. Model-based optoacoustic inversion with arbitrary-shape detectors. *Medical physics*. 2011;38:4285-95.
22. Chan TF and Vese LA. Active contours without edges. *IEEE transactions on image processing : a publication of the IEEE Signal Processing Society*. 2001;10:266-77.
23. Bonetti PO, Lerman LO and Lerman A. Endothelial dysfunction: a marker of atherosclerotic risk. *Arteriosclerosis, thrombosis, and vascular biology*. 2003;23:168-75.
24. Cosentino F, Rubattu S, Savoia C, Venturelli V, Pagannonne E and Volpe M. Endothelial dysfunction and stroke. *Journal of cardiovascular pharmacology*. 2001;38 Suppl 2:S75-8.
25. Shi Y and Vanhoutte PM. Macro- and microvascular endothelial dysfunction in diabetes. *J Diabetes*. 2017;9:434-449.
26. Liao F, Burns S and Jan YK. Skin blood flow dynamics and its role in pressure ulcers. *J Tissue Viability*. 2013;22:25-36.
27. Cracowski JL, Minson CT, Salvat-Melis M and Halliwill JR. Methodological issues in the assessment of skin microvascular endothelial function in humans. *Trends in pharmacological sciences*. 2006;27:503-8.
28. Cross TJ and Sabapathy S. The impact of venous occlusion per se on forearm muscle blood flow: implications for the near-infrared spectroscopy venous occlusion technique. *Clinical physiology and functional imaging*. 2017;37:293-298.
29. Wilkinson IB and Webb DJ. Venous occlusion plethysmography in cardiovascular research: methodology and clinical applications. *British journal of clinical pharmacology*. 2001;52:631-46.
30. Spiro JR, Digby JE, Ghimire G, Mason M, Mitchell AG, Ilsley C, Donald A, Dalby MC and Kharbanda RK. Brachial artery low-flow-mediated constriction is increased early after coronary intervention and reduces during recovery after acute coronary syndrome: characterization of a recently described index of vascular function *Eur Heart J*; 2011(32): 856-66.
31. Corretti MC, Anderson TJ, Benjamin EJ, Celermajer D, Charbonneau F, Creager MA, Deanfield J, Drexler H, Gerhard-Herman M, Herrington D, Vallance P, Vita J and Vogel R. Guidelines for the ultrasound assessment of endothelial-dependent flow-mediated vasodilation of the brachial artery: a report of the International Brachial Artery Reactivity Task Force. *Journal of the American College of Cardiology*. 2002;39:257-65.
32. Tzoumas S, Nunes A, Olefir I, Stangl S, Symvoulidis P, Glasl S, Bayer C, Multhoff G and Ntziachristos V. Eigenspectra optoacoustic tomography achieves quantitative blood oxygenation imaging deep in tissues. *Nat Commun*. 2016;7:12121.

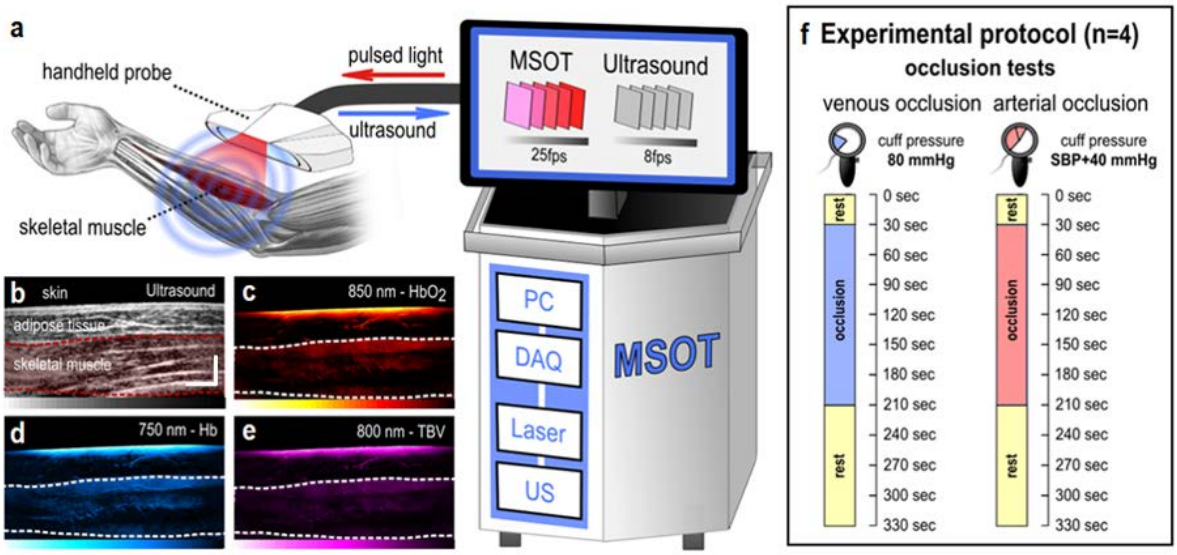

Figure 1. System principle of operation and experimental protocol. (a) Hybrid clinical MSOT/Ultrasound employs a handheld probe for real-time multispectral image acquisition of the skeletal muscles in the human forearm (wavelength range: 700 to 970 nm). (b) Ultrasound image of the human forearm: The skin surface, the subcutaneous adipose tissue and the muscle regions (light red region) are tagged. Scale bars: 1 cm. MSOT image of the forearm region acquired (c) at 850 nm, where HbO_2 (oxygenated hemoglobin) light absorption is significantly higher compared to Hb (deoxygenated hemoglobin), (d) at 750 nm, where Hb light absorption is significantly higher compared to HbO_2 and (e) at 800 nm, where HbO_2 light absorption equals that of Hb (isosbestic point which represents the TBV: total blood volume). The white dotted line marks the measured muscle area. (f) The experimental protocol followed for the occlusion tests on the four participating subjects. DAQ: Data acquisition card, SBP: Systolic blood pressure.

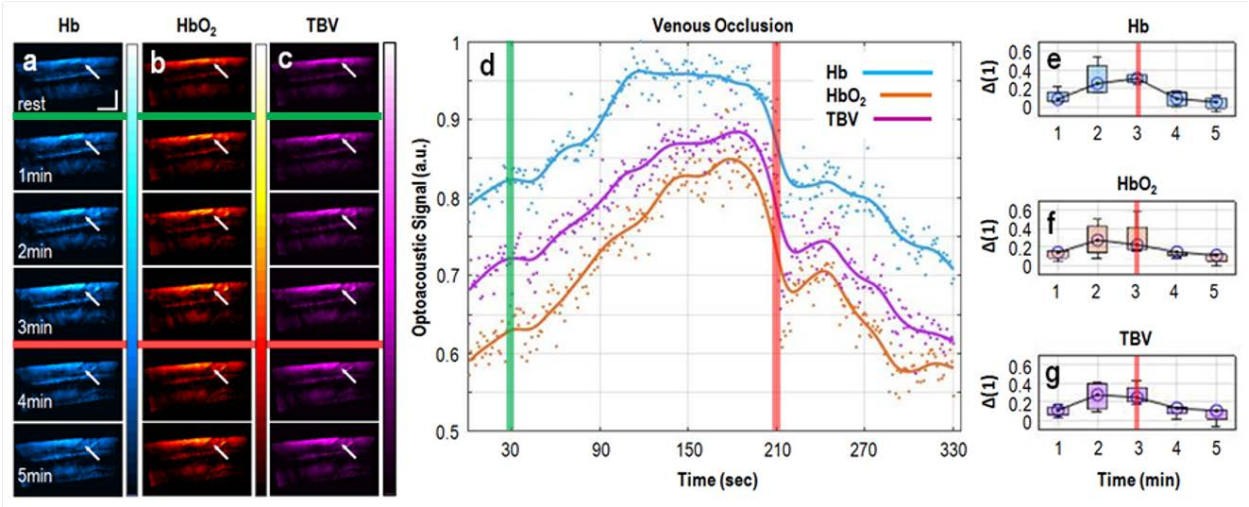

Figure 2. MSOT imaging of the forearm muscle hemodynamics and oxygen kinetics during venous occlusions. The whole process lasts 5.5 min: 0.5 min of baseline measurement, 3 min of cuff-induced venous occlusion and 2 min measurement after cuff deflation. Representative image series of (a) Hb-distribution (MSOT at 750nm), (b) HbO_2-distribution (MSOT at 850nm) and (c) TBV-distribution (MSOT at 800nm) within the segmented muscle area at different time points of the venous occlusion challenge (Subject 3). The white arrows point to the muscle region where the changes are more prominent. Scale bars: 1 cm. (d) Representative time plot (smoothing splines) of the mean optoacoustic signal for Hb, HbO_2 and TBV within the segmented muscle area over the whole venous occlusion challenge (Subject 1). Box plot of the mean change of (e) Hb, (f) HbO_2 and (g) TBV optoacoustic signal within the muscle for each minute of the venous occlusion challenge, with regard to the corresponding baseline value for

all (n=4) subjects. The green thin stripe corresponds to the time point of cuff inflation. The red stripe corresponds to the time point of the cuff deflation.

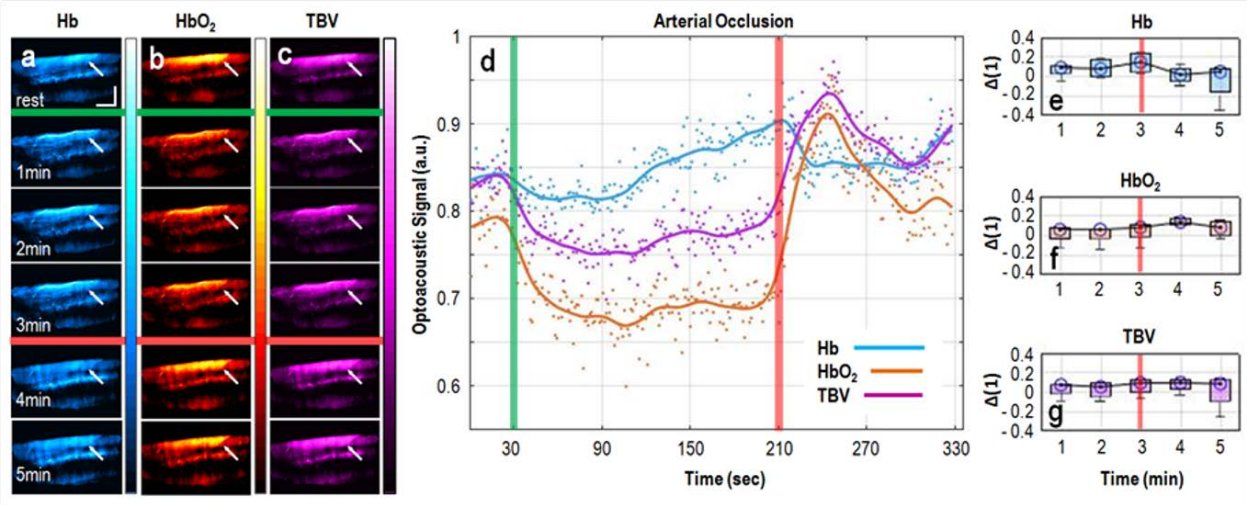

Figure 3. MSOT imaging of the forearm muscle hemodynamics and oxygen kinetics during arterial occlusions. The whole process lasts 5.5 min: 0.5 min of baseline measurement, 3 min of cuff-induced arterial occlusion and 2 min measurement after cuff deflation. Representative image series of (a) Hb-distribution (MSOT at 750nm), (b) HbO_2-distribution (MSOT at 850nm) and (c) TBV-distribution (MSOT at 800nm) within the segmented skeletal muscle area at different time points of the arterial occlusion challenge (Subject 3). The white arrows point to the muscle region where the changes are more prominent. Scale bars: 1 cm. (d) Representative time plot (smoothing splines) of the mean optoacoustic signal for Hb, HbO_2 and TBV within the segmented muscle area over the whole arterial occlusion challenge (Subject 1). Box plot of the mean change of (e) Hb, (f) HbO_2 and (g) TBV optoacoustic signal within the muscle for each

minute of the arterial occlusion challenge, with regard to the corresponding baseline value for all (n=4) subjects. Even if the HbO_2 signal in (f) remains relatively stable during the arterial occlusion, as in a low flow and not in a complete ischemia state, the hyperemic reaction after the cuff deflation is still clear. The green thin stripe corresponds to the time point of cuff inflation. The red thin stripe corresponds to the time point of cuff deflation.